CHEMPHYSCHEM

Supporting Information

Spatially Selective Heteronuclear Multiple-Quantum Coherence Spectroscopy for Biomolecular NMR Studies

Bharathwaj Sathyamoorthy,[a, c] David M. Parish,[a] Gaetano T. Montelione,[b] Rong Xiao,[b] and Thomas Szyperski*[a]

cphc_201301232_sm_miscellaneous_information.pdf

(1) NMR acquisition parameters

(2) ^{1}H T_1 relaxation in the presence of additional 180^{o} pulses

(3) m_c and m_{SS} as a function of t_1 evolution time and resulting line-broadening along ω_1 in SS HMQC with n = 4 slices as a function of T_1

(4) Contour plots of conventional 2D HMQC spectra

(1) NMR acquisition parameters

Table S1 SS HMQC NMR spectra acquired for the present study.

Protein [conc.; temp.; τ_c[a]; $T_{1,CH3}$[b]; $T_{1,NH}$[b]]	excitation (c/ SS)	HMQC type[c] (sim/ct)	spectral widths $^1H;^{13}C/^{15}N$ (ppm)	number of real points[d] $^1H;^{13}C/^{15}N$	carrier position $^{13}C;^{15}N$ (ppm)	num-ber of scans	$t_{measure}$ (mins)[e]	SS Detec-tion yield[f] $^{13}C/\ ^{15}N$ (%)
Ubiquitin [3.7 mM; 25 °C; 4.5 ns; *500±100 ms; 800±100 ms*]	c	sim	11.6; 12.7/31.6	512; 78	19.6; 115.5	32	23	-
		ct	11.6; 12.7	512; 67	21.5	32	17.6	-
	SS	sim	11.6; 12.7/31.6	512; 78	19.6; 115.5	32	23 (**1.5**)	100/97
		ct	11.6; 12.7	512; 67	21.5	32	17.6 (**1.1**)	100
GmR137 [0.7 mM; 20 °C; 5.0 ns; *600±100 ms; 1400±500 ms*]	c	sim	12.0; 9.0/22.4	512; 55	23.8; 119.0	32	16	-
		ct	12.0; 22.4	512; 47	23.8	16	5.9	-
	SS	sim	12.0; 9.0/22.4	512; 55	23.8; 119.0	32	16 (**2.0**)	100/96
		ct	12.0; 22.4	512; 47	23.8	16	5.9 (**0.75**)	97
MBP [1.0 mM; 20 °C; 23.3 ns; *650±150 ms; -- ms*]	c	ct	14.0;19.1	512; 100	26.1	32	24	-
	SS	ct	14.0;19.1	512; 100	26.1	32	24 (**1.5**)	97

[a] τ_C represents the isotropic rotational correlation time estimated from the ratio of average polypeptide backbone ^{15}N T_1 and T_2 relaxation times

[b] $T_{1,CH3}$ and $T_{1,NH}$ represent the average T_1 relaxation times of methyl and amide protons, respectively

[c] Inter-scan delays (d1 + d_{WET} + $t_{2,max}$) for sim- and *ct*-HMQC experiments were 230 and 180 ms, respectively, with d_{WET} = 20 ms and $t_{2,max}$ = 59 ms

[d] $t_{1,max}$ for sim- and *ct*-HMQC experiments were 64 and 28 ms, respectively. The ^1H carrier was set to resonance of the water line

[e] The measurement times for the rapidly acquired spectra shown in Figure 7 data are provided in bold and in parenthesis

[f] SS HMQC Peak yields are in percent and relative to the number of peaks observed in conventional HMQC with the same measurement time. They are the same for the SS HMQC spectra recorded with both long and short (Figure 7) measurement times (see text)

(2) ^{1}H T_1 relaxation in the presence of additional 180^o pulses

Figure S1 compares the ^{1}H r.f. pulse schemes for conventional (A) and SS HMQC implemented with n = 4 slices (B), considering also the relaxation delays before excitation. For additional details and the definition of delays, see Figure 2 and text.

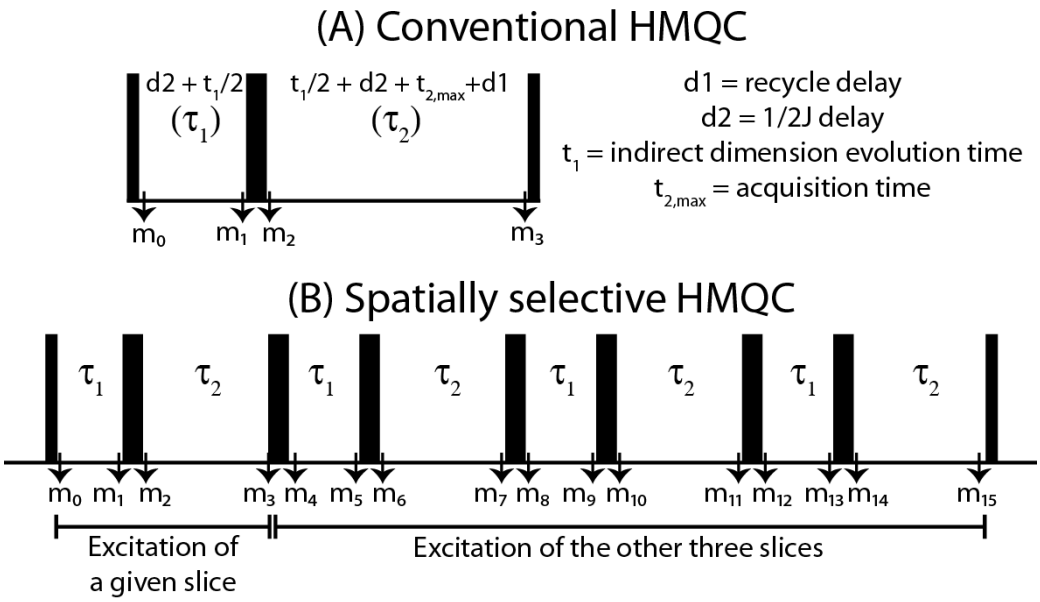

Figure S1: Salient features of ^{1}H r.f. pulse schemes governing ^{1}H T_1 relaxation between detection of FIDs. **(A)** conventional HMQC. **(B)** SS HMQC implemented with n = 4 slices.

(A) ^{1}H T_1 relaxation in conventional HMQC yielding m_c

$$m_{t+1} = 1 + (m_t - 1)\exp\left(-\frac{t}{T_1}\right)$$

$$m_0 = 0$$

$$m_1 = 1 - \exp\left(-\frac{\tau_1}{T_1}\right)$$

$$m_1 = 1 - A \text{ where } A = \exp\left(-\frac{\tau_1}{T_1}\right)$$

$$m_2 = -m_1$$

$$m_2 = -(1 - A)$$

$$m_3 = 1 + (m_2 - 1)\exp\left(-\frac{\tau_2}{T_1}\right)$$

$$m_3 = 1 - (2 - A)B \text{ where B} = \exp\left(-\frac{\tau_2}{T_1}\right)$$

$$m_3 = 1 - 2B + AB$$

$$m_C = 1 - 2B + AB$$

(B) ^{1}H T_1 relaxation in SS HMQC with n = 4 slices yielding m_{SS}

$$m_3 = 1-(2-\mathrm{A})B$$
$$m_4 = -[1-(2-A)B]$$
$$m_5 = 1-[2-(2-A)B]A$$
$$m_6 = -\{1-[2-(2-A)B]A\}$$
$$m_7 = 1-\{2-[2-(2-A)B]A\}B$$
$$m_8 = -(1-\{2-[2-(2-A)B]A\}B)$$
$$m_9 = 1-(2-\{2-[2-(2-A)B]A\}B)A$$
$$m_{10} = -[1-(2-\{2-[2-(2-A)B]A\}B)A]$$
$$m_{11} = 1-[2-(2-\{2-[2-(2-A)B]A\}B)A]B$$
$$m_{12} = -\{1-[2-(2-\{2-[2-(2-A)B]A\}B)A]B\}$$
$$m_{13} = 1-\{2-[2-(2-\{2-[2-(2-A)B]A\}B)A]B\}A$$
$$m_{14} = -(1-\{2-[2-(2-\{2-[2-(2-A)B]A\}B)A]B\}A)$$
$$m_{15} = 1-(2-\{2-[2-(2-\{2-[2-(2-A)B]A\}B)A]B\}A)B$$
$$m_{SS} = 1-(2-\{2-[2-(2-\{2-[2-(2-A)B]A\}B)A]B\}A)B$$
$$m_{SS} = 1-2B+2AB-2AB^2+2A^2B^2-2A^2B^3+2A^3B^3-2A^3B^4+A^4B^4$$
$$m_{SS} = 1+2\sum_{i=0,1,2,3} B^{i+1}\left(A^{i+1}-A^i\right)-A^4B^4$$
$$A = \exp\left(-\frac{\tau_1}{T_1}\right) \qquad B = \exp\left(-\frac{\tau_2}{T_1}\right)$$

One thus obtains

$$\rho = \frac{m_{SS}}{m_C} = \frac{1 + 2\sum_{i=0,1,2,3} B^{i+1}\left(A^{i+1} - A^{i}\right) - A^4 B^4}{1 - 2B + AB}$$

$$\text{where A} = \exp\left(-\frac{\tau_1}{T_1}\right) \quad B = \exp\left(-\frac{\tau_2}{T_1}\right)$$

$\rho(0)$ is calculated with

$$t_1 = 0\,ms;\; d2 = \frac{1}{2 \times 110} = 4.54\;ms; t_{2,\max} = 59\,ms;\; d1 = 170\;\left(d_{WET} = 20\,ms\right)$$

$$\tau_1 = d2 + \frac{t_1}{2} = 4.54\,ms$$

$$\tau_2 = \frac{t_1}{2} + d2 + t_{2,\max} + d1 = 233.54\,ms$$

Figure S2 shows a plot of ρ(t_1 = 0) = m_{SS}/m_c as a function of ^{1}H T_1 given the delays chosen for the present implementations (see also Figure 2 and text).

For T_1 = 0, ρ(t_1 = 0) = 1 because m_c = m_{SS} = 1, that is, the steady state magnetization present when the 90^o pulse is applied equals the magnetization in thermal equilibrium.

For T_1 → ∞, ρ(t_1 = 0) → 4 because the four slices of the SS HMQC experiment experience a four-fold longer delay for T_1-relaxation while the effect of the additional 180^o pulses separated by the short delay d2 becomes negligible.

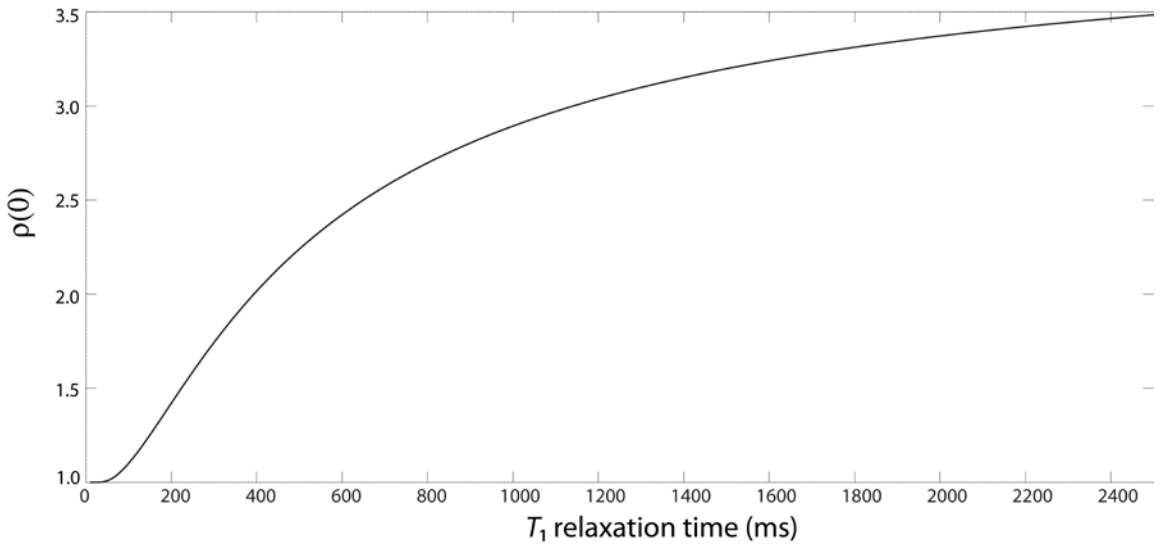

Figure S2. Plot of ρ(t_1 = 0) *versus* ^{1}H T_1

(3) m_c and m_{SS} as a function of t_1 evolution time and resulting line-broadening along ω_1 in SS HMQC with n = 4 slices as a function of T_1

Figure S3 shows selected plots of m_c and m_{SS} as a function of t_1 evolution time in (A) and the resulting small line broadening for SS HMQC implemented with n = 4 slices as a function of ^{1}H T_1 in (B). Calculations were performed with the delays chosen for the present study (Table S1; Figure 2, see also above).

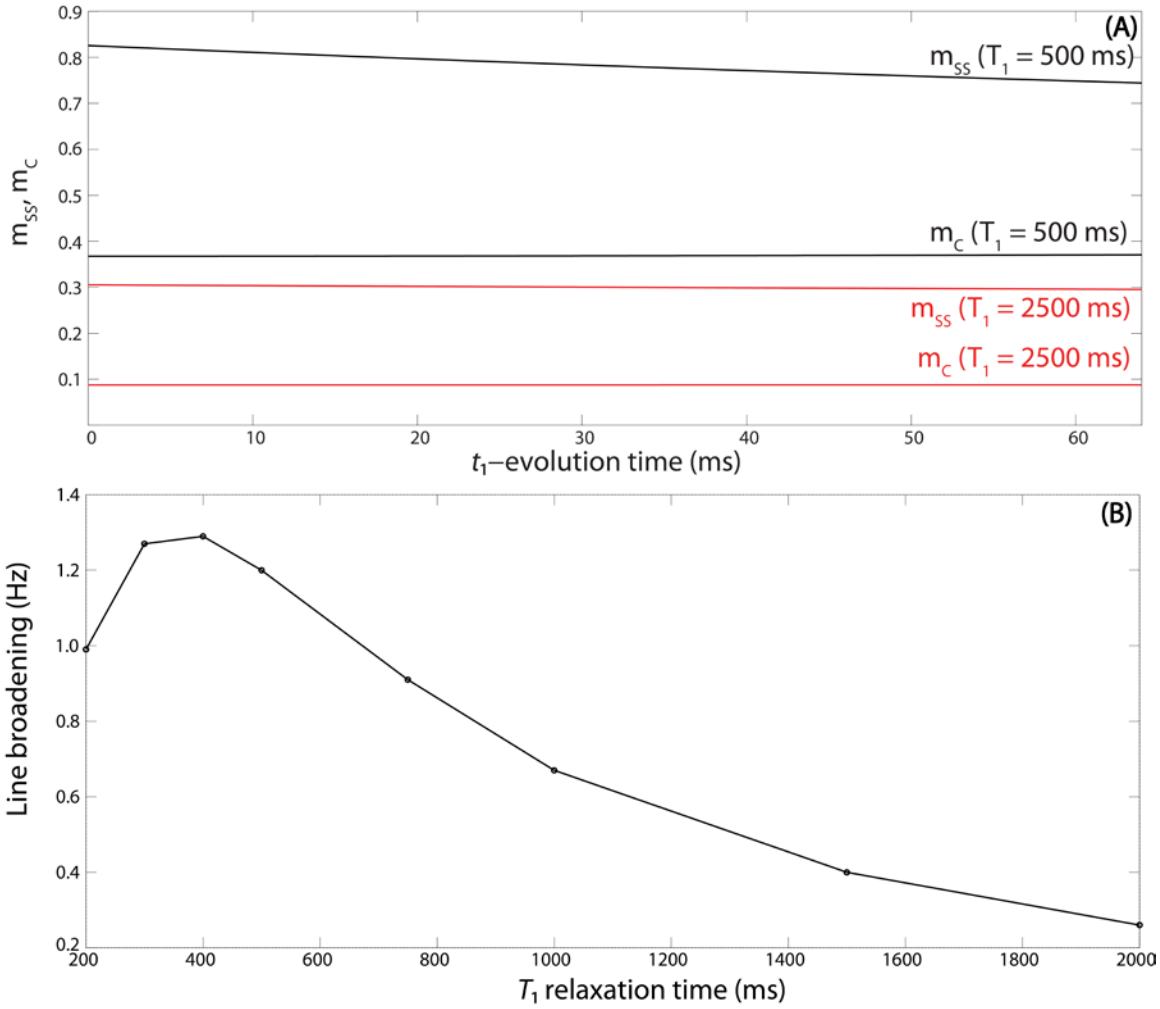

Figure S3. (A) Plots of m_c and m_{SS} versus t_1 for two different ^{1}H T_1 values. (B) Line broadening in SS HMQC *versus* T_1 obtained by fitting a mono-exponential function to plots for different T_1 values as shown in (A) for two selected T_1 values.

(4) Contour plots of conventional 2D HMQC spectra

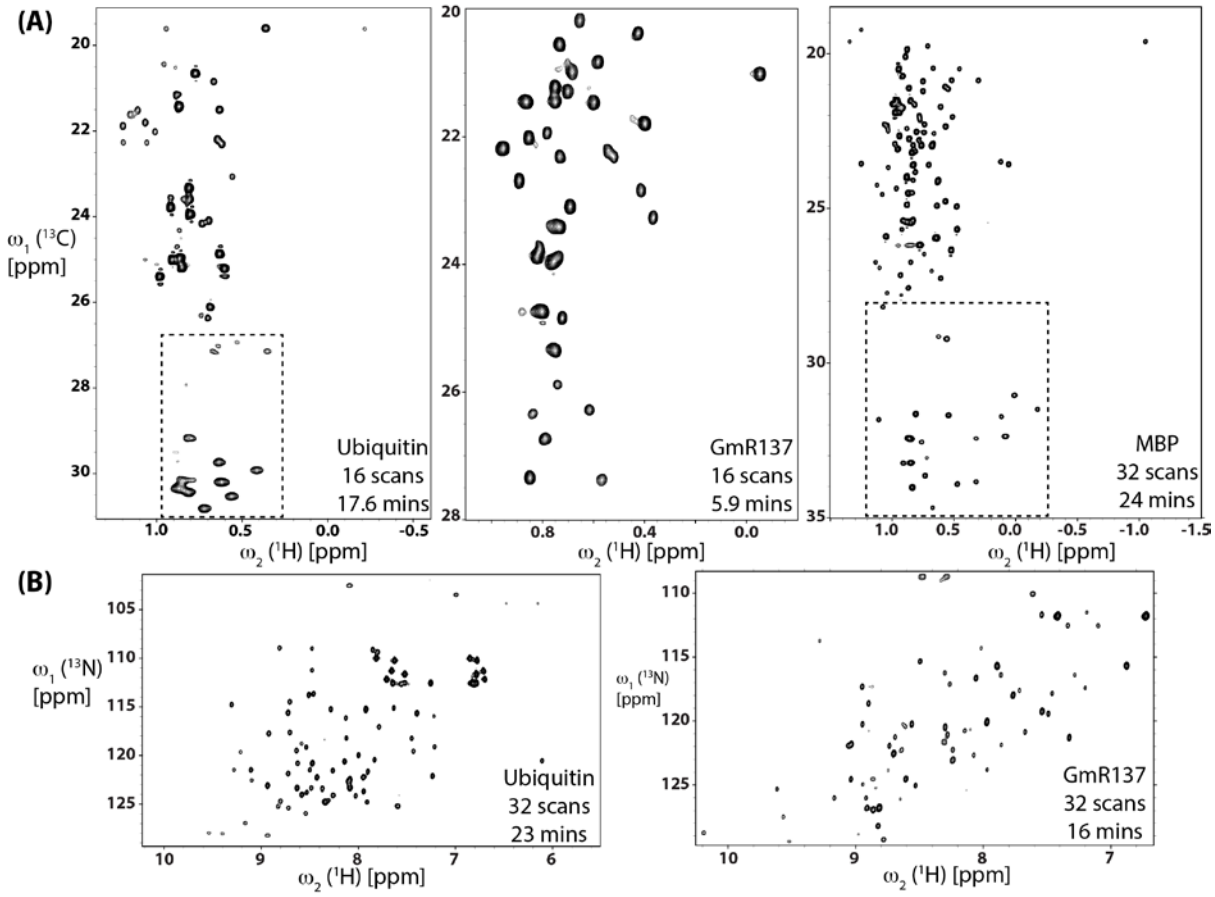

Figure S4. Conventional HMQC spectra (for acquisition parameters, see Table S1). (A) *ct*-HMQC spectra acquired for proteins ubiquitin, GmR137 and MBP (boxed spectral regions contain folded peaks). (B) Spectral regions containing polypeptide backbone NH signals of sim-HMQC spectra acquired for proteins ubiquitin and GmR137.